Eur Biophys J (2003) 32: 329–341
DOI 10.1007/s00249-003-0283-1

ARTICLE

F. Boffi · I. Ascone · S. Della Longa · M. Girasole
G. Yalovega · A.V. Soldatov · A. Varoli-Piazza
A. Congiu Castellano

X-ray absorption near-edge spectroscopy of transferrins: a theoretical and experimental probe of the metal site local structure

Received: 24 May 2002 / Revised: 17 December 2002 / Accepted: 19 December 2002 / Published online: 28 February 2003

Abstract Proteins of the transferrin (Tf) family have a role in metal transport in vertebrates and have been extensively studied. The results here reported provide, for the first time, a detailed systematic comparison of metal sites in Tf complexes involving several atoms in the whole protein and in two different types of Tfs. The high interest in the structural variations induced in a metalloprotein upon the uptake of different metals is related to the hypothesis of the metals' involvement in some neuropathologies. We propose a comparative study of the X-ray absorption spectra at the K-edge of iron, copper, zinc and nickel in serotransferrin and ovotransferrin. The experimental data are simulated using an algorithm of the full multiple scattering method. Our results show that: (1) the local structure of each site (N-terminal and C-terminal) is correlated to the ligation state of the other site; (2) the difference between the two proteins is related to site local structure and depends on the metal ion nature being greater in the case of copper and zinc with respect to iron and nickel ions; (3) X-ray spectroscopy is confirmed as a suitable technique able to discriminate between coordination models proposed by X-ray diffraction.

F. Boffi · A. Varoli-Piazza · A. Congiu Castellano (✉)
Dipartimento di Fisica and INFM, Università "La Sapienza",
Piazzale A. Moro 2, 00185 Rome, Italy
E-mail: a.congiu@caspur.it

I. Ascone
LURE, CNRS, Commissariat a l'Energie Atomique,
MEN, Bâtiment 209D, 91405 Orsay, France

S. Della Longa
Dipartimento di Medicina Sperimentale and INFM,
Università de L'Aquila, 67100 L'Aquila, Italy

M. Girasole
ISM-CNR, Via Fosso del Cavaliere,
00133 Rome, Italy

G. Yalovega · A.V. Soldatov
Faculty of Physics, Rostov State University,
5 Sorge, 344090 Rostov-Don, Russia

Keywords Proteins · Structure · Transferrins · X-ray absorption near-edge spectroscopy

Abbreviations MS: multiple scattering · Tf: transferrin XANES: X-ray absorption near-edge structure

Introduction

The transferrins are a homogeneous group of glycoproteins widely distributed in the extracellular fluids of vertebrates (Aisen et al. 1978; Aisen 1989; Baker and Lindley 1992). These proteins have the following common physicochemical and biological properties: they are made of a single polypeptide chain of MW around 80 kDa organized in two similar, but not identical, iron-binding sites disposed in the N-terminal and C-terminal halves of the molecule, respectively. Transferrins reversibly bind two Fe^{3+} ions and the binding depends on concomitant synergistic binding of carbonate (or bicarbonate) anions that bridge between the metal and the protein. All transferrins are recognized by specific membrane receptors (Legrand et al. 1988; Crichton 1991). The transferrin single polypeptide chain results from the duplication of the gene of an ancestral protein transferrin with half the molecular weight and only one iron-binding site (Williams 1975, 1982).

In this work, two members of the transferrin family have been investigated: the human serotransferrin from blood plasma and the hen ovotransferrin from avian egg white. The serotransferrin has a specific role in iron transport in vertebrates and is capable of delivering iron to cells by receptor-mediated endocytosis, in a process referred to as the transferrin cycle. It has been proposed that transferrins may transport other metal ions and deposit them in the cell (Grossman et al. 1993). The cells in the brain possess a specific high-affinity receptor for transferrin (Roskams and Connor 1990) that is independent of the transported metal. The interaction between transferrin and its receptor may act as a general metal ion regulatory system in the central nervous

system, extending beyond its postulated role in iron regulation (Bali and Aisen 1991; Evans et al. 1994).

Ovotransferrin has an antibacterial function: its ability to bind iron tightly can inhibit the growth of some bacteria and contributes to the defence of the cell against infection. Moreover, a recent study on the crystal structure of Fbp, an iron uptake protein from pathogenic bacteria of *Haemophilus influenzae* (Bruns et al. 1997), reveals an element homologous to a single lobe of the transferrin structure.

Previous X-ray crystallographic studies of serotransferrin and ovotransferrin (Bayley et al. 1988; Anderson et al. 1989; Lindley et al. 1993) have determined the three-dimensional structure of the protein and the stereochemistry of the iron-binding site. On the basis of these results, a model has been proposed in which the iron is hexacoordinated to two Tyr, one His and one Asp residues and to a (bi)carbonate linked to an Arg residue. An extended X-ray absorption fine structure (EXAFS) study on iron-bound serotransferrin fragments (Garrat et al. 1986) provided bond distances with an error of 0.02 Å between the ion and its ligands. A more recent X-ray absorption study (Garrat et al. 1991) on Cu-ovotransferrin indicated a different organization of the ligands around the ion in the two sites, at variance with the reported identity of both sites in their complex with iron ions.

Actually, the two sites of transferrin show great homologies but they are not identical. Differences between the sites have been brought out by many physicochemical studies. Thermodynamic constants for the binding of iron to transferrin show a greater affinity for the C-site than the N-site (Kretchmar and Raymond 1986); transferrin site behaviour depends on pH, one iron being removed between pH 7 and 5.5 while the other is lost between pH 5.5 and 4, implying that one of the two sites is relatively acid stable and the other is relatively acid labile (Baldwin and De Sousa 1982). Studies on transferrin show that other metal ions like Zn, Cu and Ni are able to bind selectively to the N-site or C-site; the affinity constant values of these metal ions for serotransferrin decrease according to the sequence Fe > Cu > Zn > Ni (Harris 1983, 1986; Hirose et al. 1996).

Small-angle X-ray scattering (SAXS) experiments on transferrin samples, without and with metal ions, show a close–open change of the active site structure, related to the presence and the nature of the metal ion (Grossmann et al. 1993, 1998) or to the pH values of the microenvironment of the protein (Congiu-Castellano et al. 1994).

Synchrotron sources provide a very intense continuum radiation that has allowed the development of X-ray absorption spectroscopy (XAS) of metalloproteins. In particular, the X-ray absorption near-edge structure (XANES) spectrum is determined by multiple scattering (MS) processes of excited inner-shell photoelectrons with the neighbouring atoms (Durham et al. 1981; Durham 1988; Natoli et al. 1990). As a consequence, the spectrum contains electronic and structural information, such as the valence state of the photo-absorber or the overall symmetry around it. We also point out that, for a reliable XANES simulation, structural information from other spectroscopic and/or structural methods such as X-ray diffraction at low resolution are required. In this way the proposed model may be refined at atomic resolution by comparing directly experimental and theoretical data; further, the use of model compounds is also helpful (Strange et al. 1987).

We present a comparative XANES study at the K-edge of iron, nickel, copper and zinc in two proteins of the transferrin family using both experimental results and an algorithm of the full MS method to simulate theoretical XANES spectra. Although the transferrin local structure has been studied, the results here reported concern, for the first time, the structure of the C- and N-terminal sites selectively filled by several metals in the whole protein. This allows us to show the dependence of one site structure on the state of the other site.

Materials and methods

Several studies report that it is possible to fill the C- or N-site of the native protein by an iron ion and to successively occupy the empty site by the desired metal ion (Zapolski and Princiotto 1980; Baldwin and De Sousa 1982; Harris 1983, 1986; Kretchmar and Raymond 1986). However, differences between the affinity constants and the percentage of occupation arise from the different methods. The affinity constants for the uptake of metal ions decrease with the succession Cu > Zn > Ni with different values for each site, and with log$K$ for the N-terminal and C-terminal sites varying from 12 to 3.

All the samples have been prepared by the method of Harris (1983, 1986), because the affinity constant of three of the four metal ions we used (Fe, Ni and Zn) have been calculated. Under these experimental conditions (high affinity constant and not complete saturation of the sites), we can conclude that a non-specific complexation of metal ions with the protein is highly improbable.

Human serum transferrin and hen ovotransferrin (Sigma, St. Louis, Mo., USA) of stated 97% purity were used without further purification. The samples in solution were freeze-dried prior to use.

Di-ligated transferrins

Di-ligated-transferrin forms were prepared by adding 3 mM chloride salts of Fe, Cu, Zn or Ni to 16 mM apotransferrin (buffer 10 mM HEPES, 5 mM $NaHCO_3$, pH 7.4) until the protein reached about 95% saturation. Differential UV spectroscopy was used to analyse the binding of metal ions to the protein for each sample at a protein concentration of 1.6×10^{-5} M.

We have monitored for all the samples the UV absorption peaks as reported elsewhere: Zn (Harris 1983) at 245 nm and 295 nm, Ni (Harris 1986) at 256 nm and 295 nm, Cu (Boffi et al. 2000) at 240 nm and 285 nm, Fe (Aisen et al. 1978) at 245 nm and 295 nm. The maximum absorption, at around 245 nm, due to Tyr, which participates in all metal ion binding, was monitored as a function of the salt added: 95% saturation was reached for di-ligated transferrins for all metal ions.

Mono-ligated transferrins

Mono-ligated transferrins, both N- and C-terminal forms (monoN-Tf and monoC-Tf, respectively), were obtained from the complete protein by saturating one of the two terminals with iron and occupying the other site with the other metal ion. We have evaluated

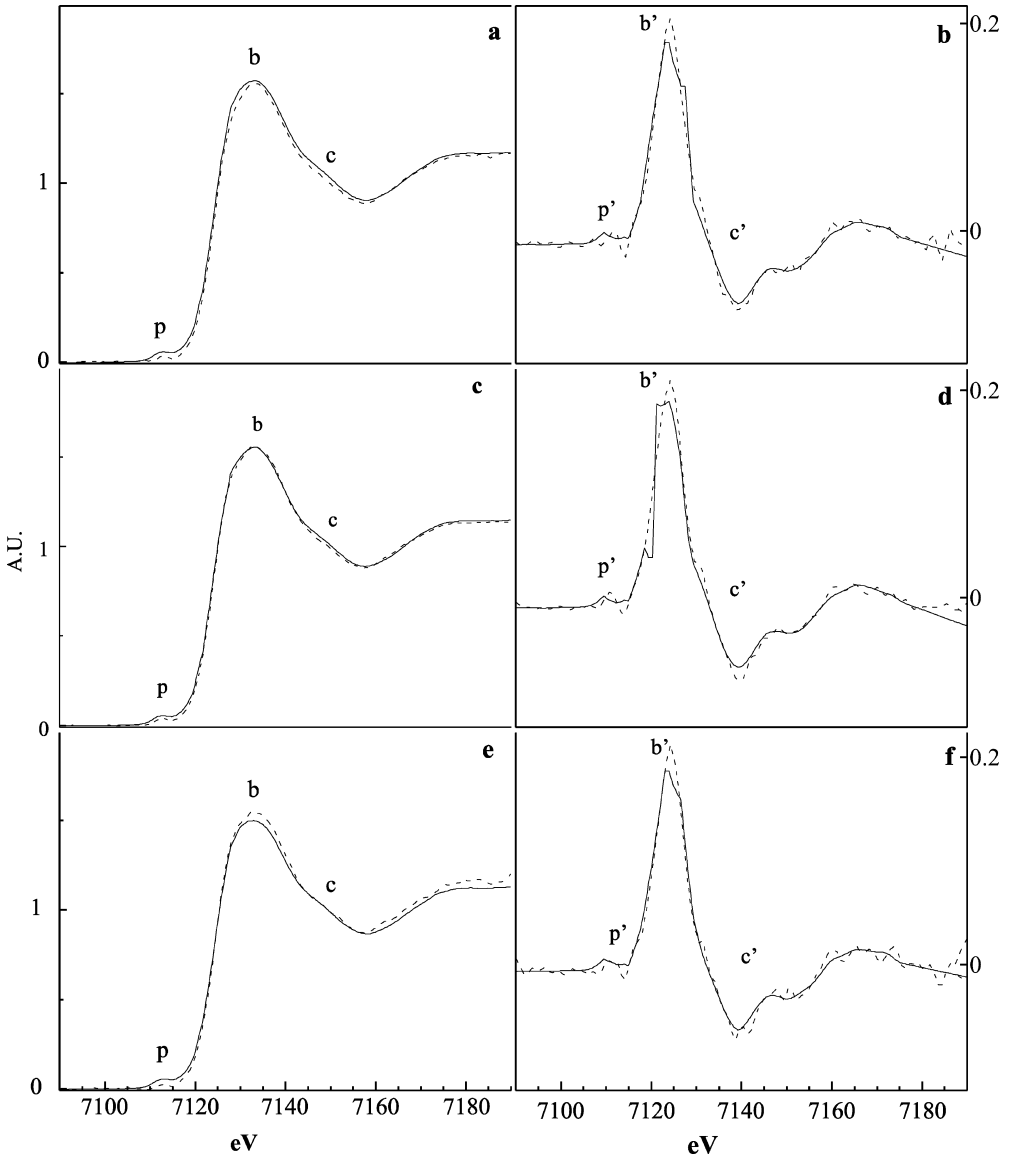

Fig. 1 Experimental XANES spectra (di-form, monoC-form, monoN-form in **a**, **c**, **e**, respectively) of serotransferrin (*solid line*), ovotransferrin (*dashed line*), and their derivative spectra (di-form, monoC-form, monoN-form in **b**, **d**, **f**, respectively) are compared in the presence of iron. XANES experiments were performed at room temperature on powder samples

the iron binding to each site by adding 1 equiv of iron to the apotransferrin solution; as a consequence, the other site was loaded by adding about 1 equiv of the other metal ion. The methods used to prepare mono-ligated transferrins are reported to yield from 80% to 90% labeling of the desired site (Harris 1986).

C-terminal transferrin

Adding one equivalent of ferrous ammonium sulfate to the whole apotransferrin molecule (buffer 10 mM HEPES, 5 mM $NaHCO_3$, pH 7.4), there is preferential oxidation and binding to the N-site of transferrin (Aisen et al. 1978). Carboxy terminal mono-Ni (Cu, Zn) transferrin was prepared by adding 3 mM of chloride salts to transferrin.

N-terminal transferrin

When one equivalent of the ferric nitrilotriacetate complex is added to the whole apotransferrin molecule (buffer 10 mM HEPES, 5 mM $NaHCO_3$, pH 7.4), there is preferential loading of the C-site (Zapolski and Princiotto 1980). N-terminal mono-Ni (Cu, Zn) transferrins were prepared by adding to the protein 3 mM of chloride salts.

XANES spectra

The K-edges of the Fe, Ni, Cu and Zn absorption spectra were collected in fluorescence mode at the D21 beam line (LURE, Orsay). A Si(311) channel-cut single crystal was used as monochromator; the energy resolution was about 1 eV. The spectra were recorded using an energy-resolving array detector made up of seven elements. Germanium of very high purity from Canberra industries (Cramer 1992) was used. The spectra (four frames with about 600 experimental points with $\Delta E = 0.2$ eV) represent a total I_f/I_0 (I_f = fluorescence count and I_0 = photon incident flux measured by a proportional counter) with a total signal averaging of 10 s/point. The fluorescence counts jumped from 70 counts/s per element before the edge (corresponding to the different K-edges for each metal ion; see Figs. 1, 2, 3, 4) to about 850 counts/s per element above the edge, giving a total count jump of about 17,500 with a noise-to-signal ratio of 10^{-4} before the edge and 2×10^{-3} after the edge. Calibration of the energy scale was achieved by measuring, at the same time as the fluorescence signal, the intensity transmitted by the appropriate metal foil. To compare the data we looked at the spectral amplitudes normalized to the respective measured atomic absorption jump (Congiu Castellano et al. 1989). In Figs. 1, 2, 3, 4 the zero on the energy scale is fixed at the first inflection point of the absorption threshold of the

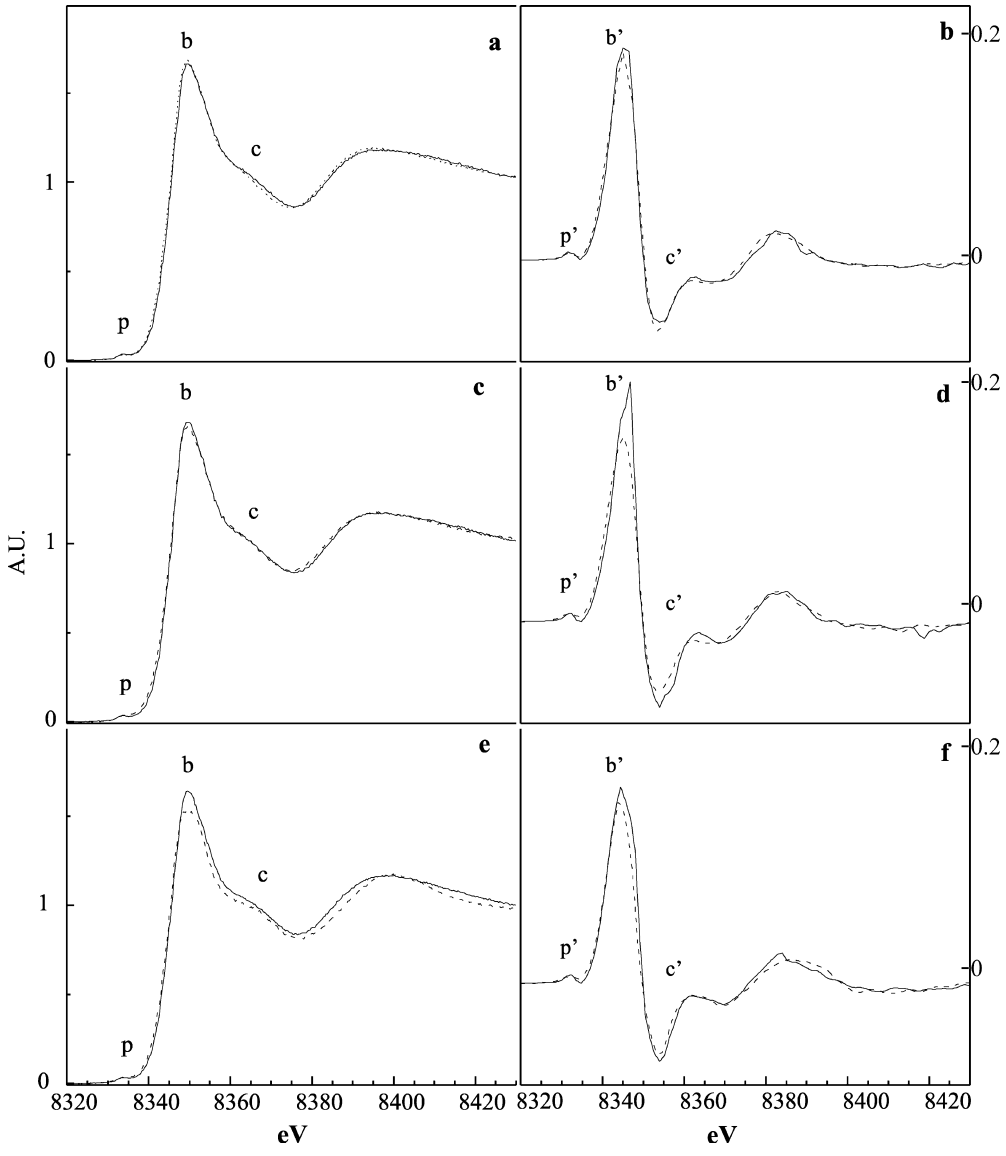

Fig. 2 Experimental XANES spectra (di-form, monoC-form, monoN-form in **a**, **c**, **e**, respectively) of serotransferrin (*solid line*), ovotransferrin (*dashed line*) and their derivative spectra (di-form, monoC-form, monoN-form in **b**, **d**, **f**, respectively) are compared in the presence of nickel. XANES experiments were performed at room temperature on powder samples

metal ion. The fitting procedures for the subtraction of the pre-edge and normalization of the spectrum cause an error in the calculated absorption jumps, and hence in the amplitude of the XANES peaks, of about 1%. The XANES spectra were collected at room temperature.

Results and discussion

The results are discussed through (1) a comparison between the two proteins serotransferrin and ovotransferrin loaded with the same metal ion, and (2) a comparison of the di-ligated, monoC- and monoN-ligated forms of each protein by varying the metal ions.

It must be underlined that XANES spectra probe the metal site structure averaged over the protein ensemble; therefore it is important that: (1) for the comparison of the two proteins, even if different percentages of C- and N-sites are loaded, this percentage is the same for both proteins; (2) we discuss the comparison between the two sites for the same protein using the XANES difference spectra between the di-form and each mono-form (N or C); only differences between the spectra greater than 0.05 au are considered meaningful, and only in this case are the differences attributed to structural differences between the two sites. Moreover, mixing of metal ions between the sites can only reduce the experimentally observed differences in the absorption spectra.

Serotransferrin and ovotransferrin comparison

In Fig. 1, XANES spectra of Fe–serotransferrin and Fe–ovotransferrin samples, recorded at the Fe K-edge, are compared. In panels a and b the XANES spectra of the dinuclear forms (both sites occupied) of the two proteins and their derivative spectra are shown, respectively; in panels c and d the XANES spectra of the monoferric C-forms (the N-site being ion free) and their derivative spectra are displayed; in panels e and f

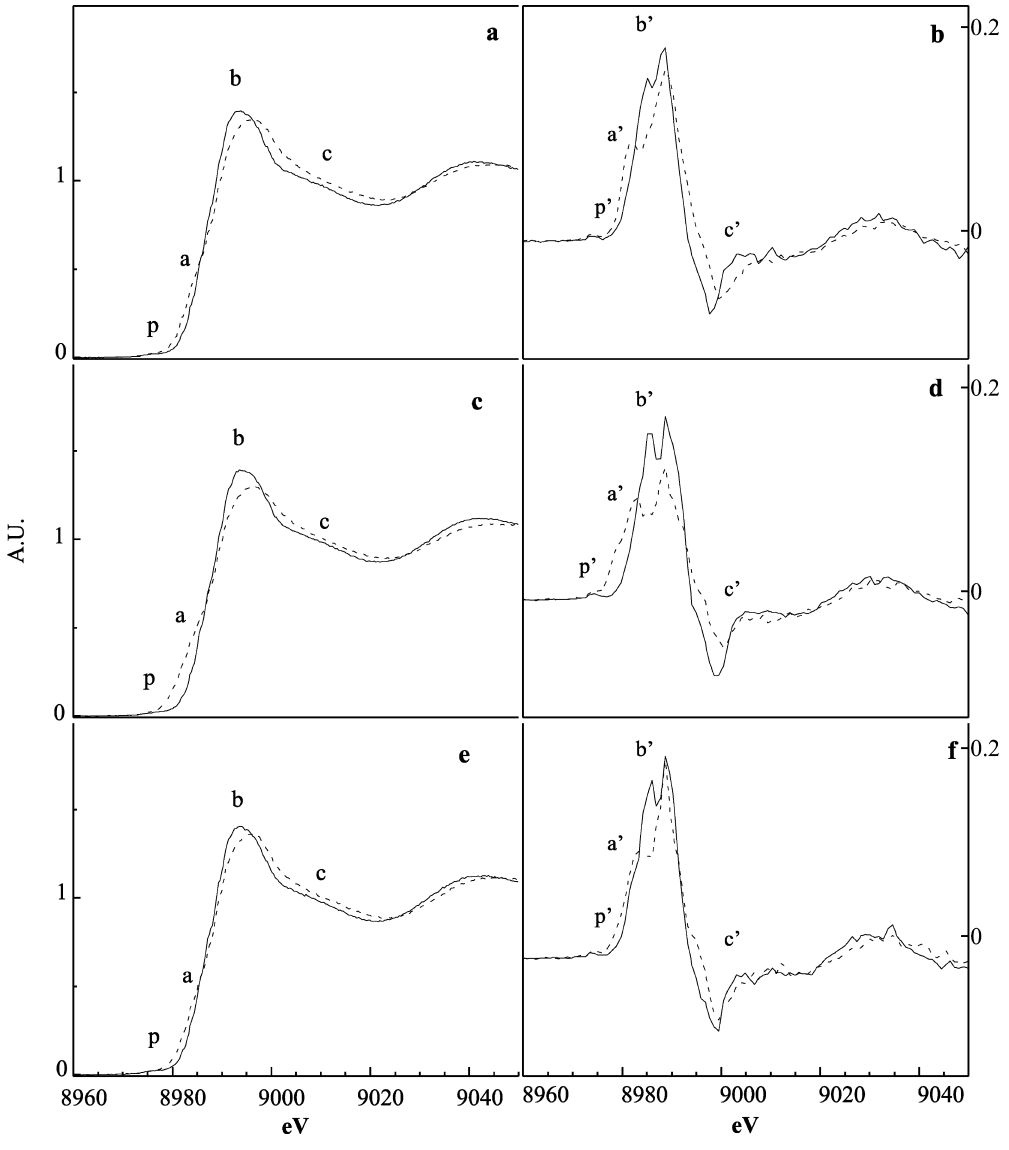

Fig. 3 Experimental XANES spectra (di-form, monoC-form, monoN-form in **a**, **c**, **e**, respectively) of serotransferrin (*solid line*), ovotransferrin (*dashed line*) and their derivative spectra (di-form, monoC-form, monoN-form in **b**, **d**, **f**, respectively) are compared in the presence of copper. XANES experiments were performed at room temperature on powder samples

the XANES spectra of the monoferric N-forms (the C-site being ion free) and their derivative spectra are shown.

In Figs. 2, 3, 4 the experimental spectra at the Ni, Cu and Zn K-edge of serotransferrin and ovotransferrin are compared in the same order: in panels a and b the XANES spectra of the dinuclear forms of the two proteins and their derivative spectra are shown, respectively; in panels c and d the XANES spectra of the monoC forms (the N-site being occupied with iron ions) and their derivative spectra are displayed; in panels e and f the XANES spectra of the monoN forms (the C-site being occupied with iron ions) and their derivative spectra are shown.

Fe–transferrins

The XANES spectra (Fig. 1) show three main features: p in the pre-edge, and b and c near the absorption edge (in the derivative spectra these are named p', b' and c'). The first weak absorption is associated with the $1s \rightarrow 3d$ transition, or alternatively with a quadrupole transitions or a $3d \rightarrow 4p$ mixing due to vibronic interactions. It was estimated that the quadrupole transitions are three orders of magnitude weaker than those observed.

The intense absorption peak (named b) about 16 eV above the first absorption was identified as the allowed transition $1s \rightarrow 4p$. The $1s \rightarrow 3d$ to $1s \rightarrow 4p$ intensity ratio is seven times larger in the tetrahedral than in octahedral coordination.

The octahedral coordination geometry of Fe^{3+} in transferrins and ovotransferrins is in agreement with crystallographic and XAS results (Bayley et al. 1988; Garrat et al. 1986). The b and c features can be explained with the MS theory.

The overall shapes of the spectra, the positions and the intensity ratio of the main features suggest a strong similarity between the proteins. EPR data (Butterworth

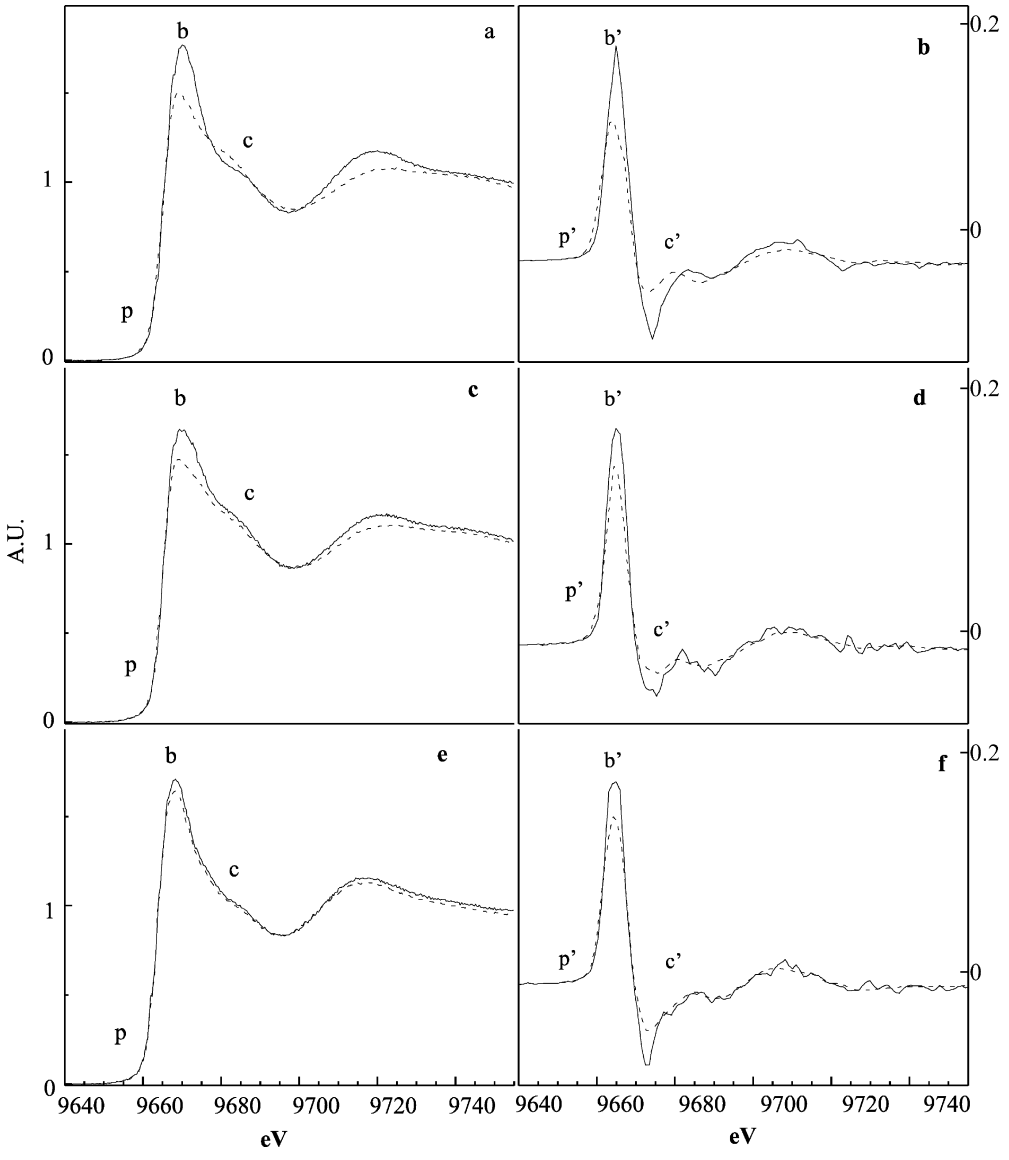

Fig. 4 Experimental XANES spectra (di-form, monoC-form, monoN-form in **a**, **c**, **e**, respectively) of serotransferrin (*solid line*), ovotransferrin (*dashed line*) and their derivative spectra (di-form, monoC-form, monoN-form in **b**, **d**, **f**, respectively) are compared in the presence of zinc. XANES experiments were performed at room temperature on powder samples

et al. 1975) on chicken ovotransferrin indicated that the signal from the diferric molecule was a composite of two distinct signals originating from the N- and C-domains of the protein; these data were interpreted by other authors (Brock 1989) in terms of structural independence of the two metal-binding sites, indicating the absence of cooperativity between the two sites.

Ni–transferrins

In Fig. 2 are compared the XANES spectra, recorded at the Ni^{2+} K-edge, of Ni–serotransferrin and Ni–ovotransferrin samples. All XANES spectra have the same features.

The MS approach shows that Ni^{2+} is coordinated in an octahedral geometry with six oxygen atoms; a similar coordination is found in NiCl XANES spectra (Clozza et al. 1986). These spectra, characteristic of octahedral geometry, show the presence of three features in the absorption edge (p, b and c). The increase of the p feature, corresponding to the 1s $\rightarrow$ 3d transition, is consistent with an increase in the amount of Ni 3d holes compared to the Cu and Zn complexes.

It has been proposed that distortions of the octahedral coordination geometry about the metal ions, imposed by the structure of the protein, destabilize Ni-transferrin with respect to the corresponding Zn-transferrin complex (Harris 1986).

Cu–transferrins

In Fig. 3, the XANES spectra of Cu–serotransferrin and Cu-ovotransferrin samples, recorded at the copper K-edge, are shown. We have discussed the features of these spectra previously (Boffi et al. 2000, 2001). A difference between the two proteins regarding the independence or the interaction among the metal sites and the geometry of the copper coordination has been shown.

XANES spectra of dinuclear serotransferrin and ovotransferrin show that the site structure of the two proteins is different. The main spectral variations concern the position of peaks a and b (identified respectively at 6 and 22 eV in the derivative spectra) as well as the overall shape of the spectra.

The geometrical arrangement of the active site in di-Cu–ovotransferrin can be still discussed in the frame of a tetragonal distorted octahedral cluster: (1) the reported red shift in the position of peak a suggests an increase in the distance between copper and its axial ligands relative to di-Cu–serotransferrin; (2) an increase in the intensity of peak c, occurring in di-Cu-ovotransferrin, can be related to a Jahn-Teller distortion (Garcia et al. 1986); (3) the blue shift and the larger broadening of the main peak b in ovotransferrin, compared with serotransferrin, suggest more disorder and a general shortening of the distances around copper relative to the equatorial ligands (Woolery et al. 1984; Alagna et al. 1986).

Zn–transferrins

Zn–serotransferrin and Zn–ovotransferrin XANES spectra at the Zn^{2+} K-edge are compared in Fig. 4. In these spectra the first weak absorption p is not present, as Zn^{2+} has no empty 3d orbital. Figure 4a and Fig. 4b show differences between di-Zn–serotransferrin and di-Zn–ovotransferrin spectra. This behaviour is due to an octahedral environment more distorted in ovotransferrin than in serotransferrin.

Summary of results

Thus our experimental results (Figs. 1, 2, 3, 4) allow a comparison between serotransferrin and ovotransferrin by varying the metal ions in the active sites:

1. The experimental spectra of the iron and nickel ligated forms (di-Fe, monoC-Fe, di-Ni, monoC-Ni) of the two proteins are quite identical; a small difference is revealed in the monoN-Fe and monoN-Ni forms.
2. In the Cu and Zn ligated forms, relevant differences between the two proteins are shown (in the di-Cu, monoC-Cu, monoN-Cu and in di-Zn, monoC-Zn forms; a smaller difference is shown in the monoN-Zn form). It is interesting to underline that the greater differences between the proteins concern the forms containing Cu and Zn ions.

Comparison of di-ligated, monoC and monoN forms of each protein by varying the metals ions

In Fig. 5 and Fig. 6 are shown the differences between the di-ligated and monoN forms, di-ligated and monoC forms, and monoN and monoC forms for serotransferrin and ovotransferrin, respectively. Only differences between spectra greater than 0.05 au are considered meaningful. The comparison between the site structure

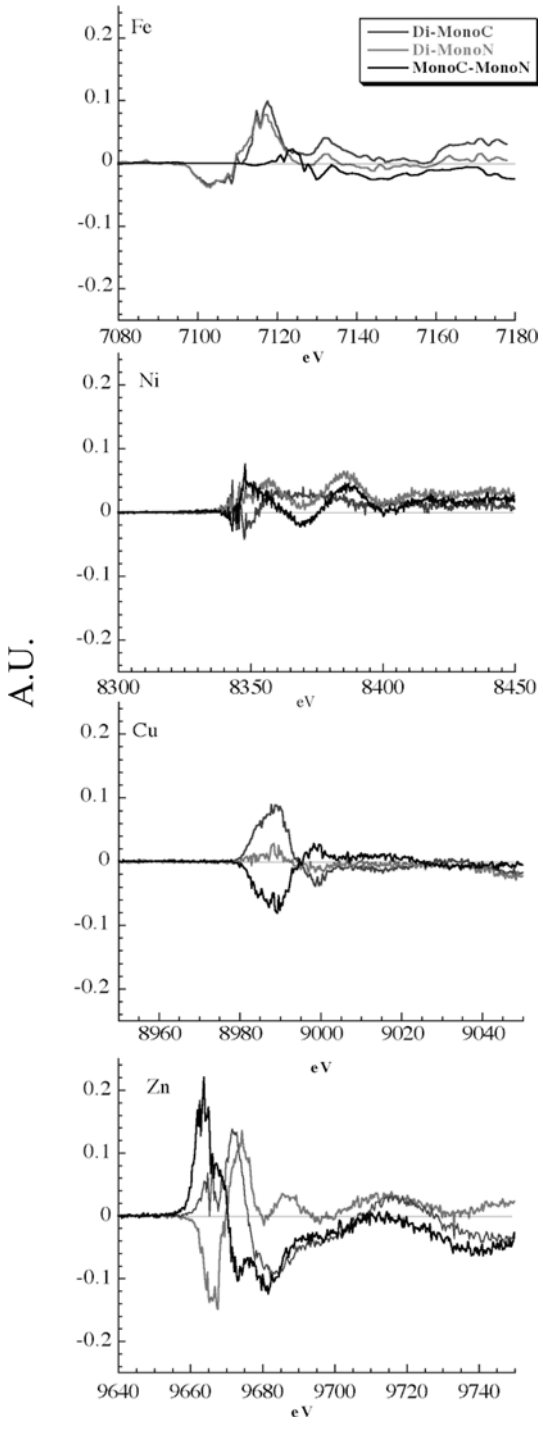

Fig. 5 Serotransferrin XANES spectral differences between di and monoN (*light grey*), di and monoC (*grey*), and monoN and monoC (*black*) forms for different metal ions

by varying the metal ions shows the characteristics described below.

Serotransferrin

For serotransferrin–Fe the monoN and monoC site structures are very similar, but the diferric form shows a

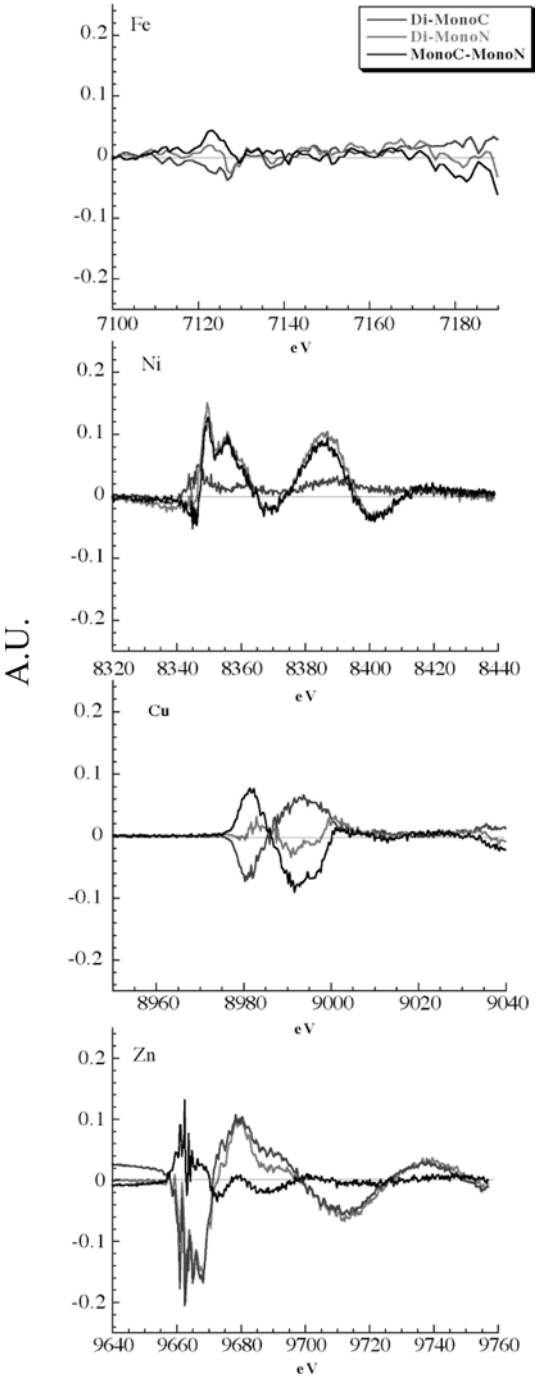

Fig. 6 Ovotransferrin XANES spectral differences between di and monoN (*light grey*), di and monoC (*grey*), and monoN and monoC (*black*) forms for different metal ions

structural site different with respect to the monoC or monoN structural site. This could be an indication of a rearrangement of the two sites following the uptake of the iron ions in both two sites and that the local structure of each site (N-terminal and C-terminal) is correlated to the ligation state of the other site. This result is not in agreement with EPR data interpretation (Brock 1989).

For serotransferrin–Ni the monoN, monoC and di-Ni forms show small differences. For serotransferrin–Cu the di-Cu and monoN forms show small differences. For serotransferrin–Zn, all the spectra show significant differences.

Ovotransferrin

For ovotransferrin-Fe, all the spectra show small differences similar to those of the Ni forms of serotransferrin. For ovotransferrin-Ni the monoC and di-Ni forms are similar while the monoN form is different. For ovotransferrin-Cu the di-Cu and monoN forms are similar. For ovotransferrin–Zn, all the spectra show significant differences.

This qualitative comparison shows that serotransferrin reveals the same behaviour with respect to ovotransferrin upon the uptake of Zn ions or Cu ions but has different behaviour upon the uptake of Fe or Ni ions.

XANES simulation

The full MS algorithm used in this study has been described previously (Della Longa et al. 1995). Atomic charge densities were obtained with the self-consistent Dirac-Slater method. Phase shifts were calculated for a molecule muffin-tin (MT) potential with touching MT spheres. XANES above the metal K-edge of metalloproteins is generated by multiple scattering of the excited photoelectron within a cluster (i.e. a group of atoms around the metal ion of the active centre), consisting of few shells of atoms (Bianconi et al. 1985).

Experimental XANES spectra have to be compared with theoretical calculations, taking into account the presence of the core hole. This process is generally treated in the frame of the $Z+1$ approximation (Durham et al. 1981; Durham 1988). Theoretical XANES simulations calculated in both the ground states and the $Z+1$ (fully relaxed) approximation, for the case of the metal K-edge XANES spectra of transferrins, do not differ significantly. Some small changes in relative intensity arise from the difference in the dipole transition matrix elements calculated in the ground state and fully relaxed potentials. This situation is almost general: for the K-edges the contribution of the core hole is rather small, while for the $L_{2,3}$ edges the core hole effect is usually significant (Soldatov et al. 1994).

In order to perform the direct comparison of XANES simulations with experimental data, the broadening of experimental spectra according to three factors must be taken into account: the core hole lifetime, the finite mean free path of the photoelectron and the experimental resolution. For the K core hole bandwidth the values of 1.25 eV (Fe), 1.44 eV (Ni) and 1.67 eV (Zn) have been used (Fuggle and Inglesfield 1992; Furenlid et al. 1995). The mean free path of the photoelectron energy-dependent function has been taken from Muller et al. (1982). For the experimental energy resolution, the value of

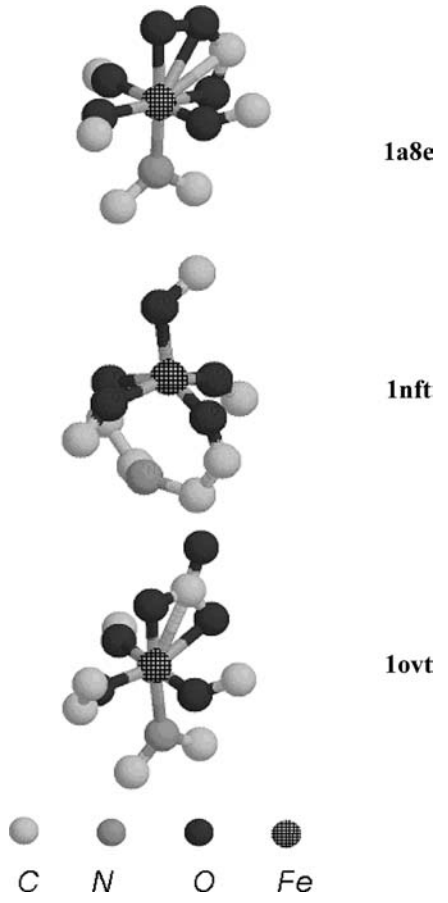

Fig. 7 Models of clusters around the active metal centre of transferrin extracted from the following PBD entries: 1a8e (Macgillivray et al., 1998), 1nft (Mizutani et al., 1999), and 1ovt (Kurokawa et al. 1995) used for XANES simulations

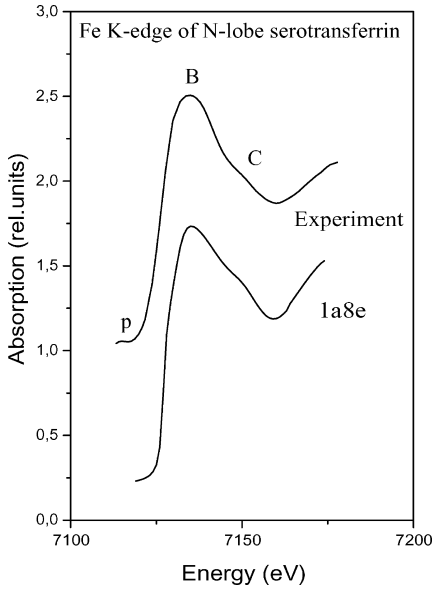

Fig. 8 Comparison of experimental Fe K-edge XANES spectra of N-lobe serotransferrin with theoretical spectra calculated for the 1a8e model from the PDB for a cluster consisting of three shells (see Fig. 7)

Table 1 Atoms taken into account in calculations according to 1a8e data (Macgillivray et al. 1998) in the three shells around the Fe ion of serum monoN transferrin

Shell number	Atom type	Radius (Å)
1	O	1.796
1	O	1.972
1	O	1.990
1	O	2.029
1	N	2.036
1	O	2.055
2	O	2.240
2	O	2.421
2	C	2.488
2	C	2.536
3	C	2.887
3	C	2.934
3	C	3.059
3	C	3.116
3	C	3.156

1.0 eV (instead of 2 eV) has been used in order to better show the characteristic features. All of these factors have been treated as contributing to the imaginary part of the self-energy term used in the calculation.

It is very difficult to obtain by X-ray diffraction a full set of coordinates with reasonable accuracy, owing to the high number of atoms in a protein molecule (Hasnain and Hodgson 1999). XAS spectroscopy is the appropriate tool to study the metal site of proteins as it gives a description of the metal sites at atomic resolution.

In Fig. 7 we present models of the transferrin metal site extracted from the following PBD (Protein Data Bank) entries: N-lobe human serotransferrin, 1a8e (Macgillivray et al. 1998); N-lobe hen ovotransferrin, 1nft (Mizutani et al. 1999); and hen diferric ovotransferrin, 1ovt (Kurokawa et al. 1995). The differences in the surroundings of the Fe_1 and Fe_2 active sites in diferric ovotransferrin are relatively small and cannot be seen in the figure. Thus, we present only one cluster for the 1ovt model. In Fig. 8 we show the comparison of the experimental Fe K-edge XANES spectrum of serum transferrin with the theoretical spectra calculated for the cluster shown in the 1a8e part of Fig. 7. The agreement between the experimental and theoretical XANES spectra obtained for the transferrin structure of Macgillivray et al. (1998) (PDB entry 1a8e) is good. The coordinates of the neighbouring atoms around the central Fe atom are given in Table 1.

An important step in the MS analyses of XANES data is to determine the size of a representative cluster which will fully reproduce the fine structure of the spectrum. The analysis of the dependence of the main structures in XANES spectra on cluster size shows that convergence with cluster size is reached for a cluster of three shells only, as the addition of the fourth shell does not result in any visible changes of the XANES spectrum. Therefore, all the next XANES calculations were performed using this cluster size.

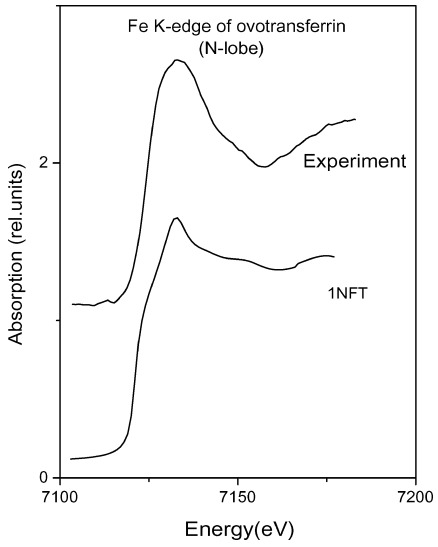

Fig. 9 Comparison of experimental Fe K-edge XANES spectra of N-lobe ovotransferrin with theoretical spectra calculated for the 1ntf model from the PDB for a cluster consisting of three shells (see Fig. 7)

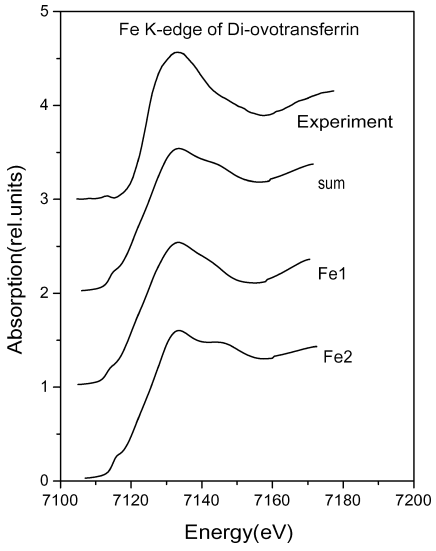

Fig. 10 Comparison of experimental Fe K-edge XANES spectra of di-ovotransferrin with theoretical spectra calculated for the 1ovt model from the PDB for the Fe_1 and Fe_2 sites, and the averaged spectrum. The cluster consists of three shells (see Fig. 7)

In Fig. 9 we present a comparison of the experimental Fe K-edge XANES spectrum of N-lobe ovotransferrin with theoretical spectra calculated for the 1ntf model from the PDB using the cluster presented in Fig. 7. As can be seen, the agreement between the spectra is worse than for the case of serotransferrin. We suppose that the reason for this is the fact that a cluster of atoms around an iron ion extracted from 1a8e PDB data describes the geometry of the active metal site in serotransferrin better than the cluster extracted from the 1ntf PDB data. Experimental Fe K-edge XANES spectra for serotransferrin and ovotransferrin are only slightly different (see Fig. 1). Thus one can expect the local geometry around the active metal site in these two types of transferrin to be quite small. On the other hand, the geometry of active metal centres extracted from the 1a8e and 1nft data sets differs significantly (see Fig. 7).

In Fig. 10 we show a comparison of the experimental Fe K-edge XANES spectrum of diferric ovotransferrin with the theoretical spectra calculated for the 1ovt model from the PDB for Fe_1 and Fe_2 active sites, together with the averaged spectrum. As one can see from Fig. 7, the cluster around the active iron site in the 1ovt model is closer to the cluster obtained from 1a8e data than the 1nft cluster. That is why the shape of the theoretical spectra is closer to the experimental spectrum for diferric ovotransferrin. In the same figure we present spectra for both Fe_1 and Fe_2 sites of diferric ovotransferrin. In spite of the differences between the Fe_1 and Fe_2 site geometries being rather small, they result in visible changes of the XANES spectral shape. This result supports again the sensitivity of XANES spectra to the fine details of local geometry around the absorbing atom.

As can be seen from Fig. 8, the agreement of the theoretical results with the experimental data obtained for serum transferrin is quite fair. However, in the case of transferrin with substituted Ni and Zn metal ions, the situation is more complicated. There are no structural data available in the literature. As a first approximation, the structure around Ni and Zn ions in transferrin has been considered as being close to the structure of Fe–Tf. In order to study the changes taking place with the substitution of an Fe ion by Ni or Zn ions, we compare (Fig. 11) normalized experimental XANES spectra at metal K-edges of Fe-, Zn- and Ni–transferrins and normalized theoretical XANES spectra, calculated for the structural model 1a8e. For all three transferrins (with Fe, Ni and Zn ions in the active centre) the same model of local geometry (see Table 1) around the active centre was used. Both experimental and theoretical spectra display the same tendency of the shape changes. For Fe–transferrin the main peak B has the lowest intensity, which increases with substitution of Fe by Ni and Ni by Zn. Both theoretical and experimental spectra show also the same tendency of the shape changes of the main rising edge. It is most sloping for Fe-Tf and the sharpest for Ni-Tf and Zn-Tf.

In the next step, we tried to vary the local structure parameters of the Ni-Tf cluster (coordinates of the first shell atoms), assuming the same symmetry of the shell. The best results were obtained when the first shell of atoms was 2% compressed (i.e. distances from Ni to the first shell of atoms were decreased by 2%; see Fig. 12). As a simulation parameter used the energy distance (ΔE) between main maximum B and high-energy minimum D. The values of ΔE are: 26.8 eV in the experimental spectrum, 24.8 eV in the theoretical spectrum of a "normal" structure (1a8e) and 26.7 eV for the structure with 2% reduced interatomic distance, respectively. This result supports the idea that substitution of Fe by a Ni

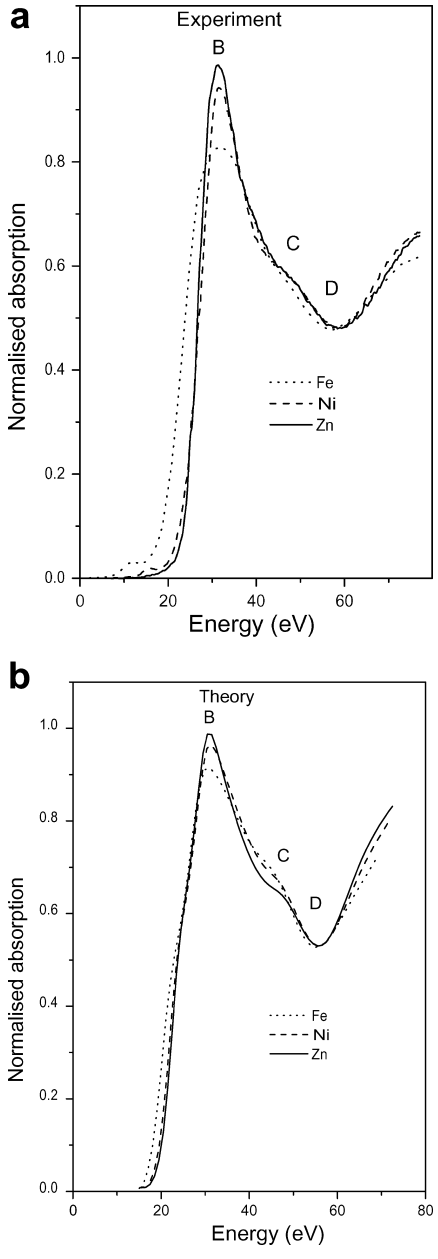

Fig. 11. **a** Normalized experimental XANES spectra at metal K-edges of Fe-, Ni- and Zn-transferrrins. **b** Normalized theoretical XANES spectra at metal K-edges of Fe-, Ni- and Zn-transferrins, calculated for structural model 1a8e from the PDB (Macgillivray et al. 1998)

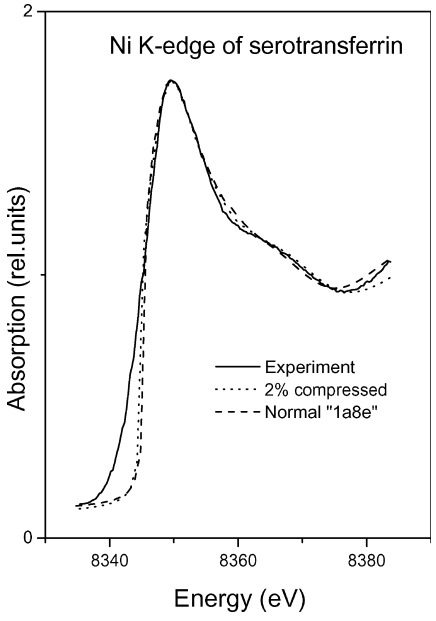

Fig. 12 Comparison of experimental and theoretical Ni K-edge XANES spectra of mono N–transferrin, calculated using the Fe–transferrin model structure and 2% compressed first-shell model

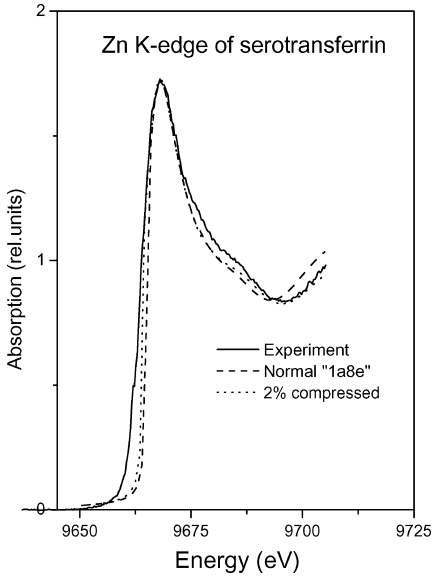

Fig. 13 Comparison of experimental and theoretical Zn K-edge XAFS of mono N–transferrin, calculated using the Fe–transferrin model structure and 2% compressed first-shell model

ion in monoN-Tf leads to a more compact surrounding of the active metal centre.

We have obtained the same result by theoretical analysis of the experimental XANES spectra (Fig. 3) of Cu–transferrins, as we have recently reported (Boffi et al. 2001). The distances of the first shell atoms around the active site (Cu ion) were found to be about 3% reduced as compared with the Fe–Tf case. This result is in qualitative agreement with an earlier EXAFS study of Cu–transferrin (Garrat et al. 1991); in that work the first shell was found to be about 5% compressed in comparison to Fe–transferrin (Cu-Tf 1.9 Å; Fe–Tf 2.0 Å). A more detailed site description could be obtained for transferrins using recent fitting programs, as has been done for azurin (Cheung et al. 2000). For Zn–transferrin the best agreement of the experimental spectra and the theoretical simulation has been obtained when the first shell of atoms around the active centre (Zn ion) has been 2% compressed as compared with Fe–Tf (see Fig. 13).

Table 2 Theoretical distances of metal ions and their neighbouring atoms obtained for Ni-, Zn- and Cu-substituted transferrins by the refinement of 1a8e data from Macgillivray et al. (1998)

	Iron (Fe^{3+}) $R_i = 0.64$ Å[a]	Nickel (Ni^{2+}) (2%) $R_i = 0.72$ Å	Copper (Cu^{2+}) (3%) $R_i = 0.69$ Å	Zinc (Zn^{2+}) (2%) $R_i = 0.74$ Å
O Tyr	1.7963	1.7604	1.7424	1.7604
O Tyr	1.9718	1.9323	1.9126	1.9323
O BCO_3	1.9905	1.9507	1.9308	1.9507
O BCO_3	2.0295	1.9889	1.9686	1.9889
N His	2.0364	1.9957	1.9753	1.9957
O Asp	2.0554	2.0143	1.9938	2.0143

These results support the idea that substitution of Fe by Zn, Cu or Ni ions in monoN–transferrin leads to more compact surroundings of the active metal centre (see Table 2).

Conclusions

The comparison between sero- and ovotransferrin spectra shows that the greater differences between the proteins' local structure concern the copper and zinc ligated forms, while there is a small difference for the iron and nickel ligated forms.

The comparison of the experimental spectra of the mono-forms and di-forms for each protein with different metal ions shows that ovo- and serotransferrins have a peculiar flexibility of monoN and monoC forms upon metal binding. We underline that only differences between the spectra greater than 0.05 au are considered meaningful. This peculiar structure modulation of the N or C site upon metal binding suggests a rearrangement of the two sites following the uptake of ions in both two sites.

The comparison of theoretical and experimental XANES spectra shows that the experimental differences observed by the substitution of Fe by Zn, Cu or Ni ions are related to reduced interatomic distances between the metal ion and the nearest neighbours, i.e. to a more compact structure of the metal site.

In spite of the approximation in XAS theory, XANES theoretical spectra are able to simulate the most important experimental structures and to discriminate among different PDB models of the transferrin iron site.

In conclusion, XANES spectroscopy is a suitable probe to reveal fine local structural differences by comparing two proteins or for each protein by varying the metal ion type.

References

Aisen P (1989) In: Loehr TM (ed) The transferrin iron carriers and iron proteins. VCH, Weinheim, pp 241–371

Aisen P, Leibam A, Zweier J (1978) Stoichiometric and site characteristic of the binding of iron to human transferrin. J Biol Chem 253:1930–1937

Alagna L, Strange RW, Durham P, Hasnain SS (1986) Stereochemisty of copper in superoxide dismutase in solution from X-ray absorption near edge structures (XANES). J Phys (Paris) C8 47:62–73

Anderson BF, Baker HM, Dodson EJ, Norris GE, Rice DW, Baker EN (1989) Structure of human lactoferrin: crystallographic structure analysis and refinement at 2.8 Å resolution. J Mol Biol 209:711–734

Baker EN, Lindley PF (1992) New perspectives on the structure and function of transferrin. J Inorg Biochem 47:147–160

Baldwin DA, De Sousa DMR (1982) The effect of pH on the kinetics of iron release from human transferrin. Biochim Biophys Acta 719:140–146

Bali P, Aisen P (1991) Receptor-modulated iron release from transferrin: differential effects on N- and C-terminal sites. Biochemistry 30:9947–9952

Bayley S, Evans R, Garrat RC (1988) Molecular structure of serum transferrin at 3.3 Å resolution. Biochemistry 27:5804–5812

Bianconi A, Congiu-Castellano A, Durham PF, Hasnain SS, Phillips S (1985) The CO bond angle of carboxymyoglobin determined by angular resolved XANES spectroscopy. Nature 318:685–687

Boffi F, Ascone I, Varoli Piazza A, Girasole M, Della Longa S, Giovannelli A, Congiu Castellano A (2000) Comparative XANES study of serotransferrin and ovotransferrin at Cu K-edge: evidence of interactions among the metal sites. Biometals 13:217–222

Boffi F, Congiu-Castellano A, Varoli-Piazza A, Della Longa S, Girasole M, Yalovega G, Soldatov AV (2001) Iron and copper K-edge XAS study of serotransferrin and ovotransferrin. J Synchrotron Radiat 8:196–198

Brock JH (1989) Iron-binding proteins. Acta Pediatr Scand Suppl 361:31–43

Bruns CM, Nowalk AJ, Arvai AS, McTigue MA, Vaughan KG, Mietzener TA, McRee DE (1997) Structure of Heamophilus influenza Fe^{3+} binding protein reveals convergent evolution within a superfamily. Nat Struct Biol 4:919–924

Butterworth RM, Gibson JF, Williams J (1975) EPR spectroscopy of iron binding fragments of hen ovotransferrins. Biochem J 149:559–563

Cheung KC, Strange RW, Hasnain SS (2000) 3D EXAFS refinement of the Cu site of structural change at the metal centre in an oxidation–reduction process: an integrated approach combining EXAFS and crystallography. Acta Crystallogr Sect D 56:697–704

Clozza A, Garcia J, Bianconi A, Corma A (1986) Local structure in bifunctional Ni-MoO_3 zeolite catalyst by K–Ni EXAFS and XANES spectroscopy. J Phys (Paris) C8 47:313–316

Congiu Castellano A, Castagnola M, Burattini E, Dell'Ariccia M, Della Longa S, Giovannelli A, Durham PJ, Bianconi A (1989) Hetereogenity of the isolated subunits of the fetal and adult human hemoglobin in solution detected by XANES spectroscopy. Biochim Biophys Acta 996:240–246

Congiu Castellano A, Barteri M, Castagnola M, Bianconi A, Borghi E, Della Longa S (1994) Structure–function relationship in the serotransferrin: the role of the pH on the conformational change and the metal ion release. Biochem Biophys Res Commun 198:646–652

Cramer SP (1988) Biochemical application of X-ray absorption spectroscopy. Wiley, New York

Cramer SP (1992) 13-element Ge detector for fluorescence EXAFS. Nucl Instrum Methods A 319:285–289

Crichton RR (1991) Chemistry and biology of the transferrin: inorganic biochemistry of iron metabolism. Horwood, Chichester, pp 101–119

Della Longa S, Soldatov AV, Pompa M, Bianconi A (1995) Atomic and electronic structure probed by X-ray absorption spectroscopy: full multiple scattering analysis with G4 XANES package. Comput Mater Sci 4:199–202

Durham PF (1988) Theory of XANES. In: Prinz R, Koningsberger D (eds) X-ray absorption: principles, applications and techniques of EXAFS, SEXAFS and XAFS. Wiley, New York, pp 53–84

Durham PJ, Pendry JB, Hodges CH (1981) XANES: determination of bond angle and multi-atom correlations in order and disordered systems. Solid State Commun 38:159–161

Evans RW, Crawley JB, Garrat RC, Grossman JG, Neu M, Aitken A, Patel KJ, Meilak A, Wong C, Singh J, Bomford A, Hasnain SS (1994) Characterization and structural analysis of a functional human serum transferrin variant and implications for receptor recognition. Biochemistry 33:12512–12520

Fuggle JC, Inglesfield JE (1992) Unoccupied electronic states. Springer, Berlin Heidelberg New York

Furenlid LR, Renner MW, Fujita E (1995) XAS studies of Ni(I), Ni(II), Ni(III) complexes. Physica B 208:739–742

Garcia J, Bianconi A, Benfatto M, Natoli CR (1986) Coordination geometry of transition metal ions in dilute solutions by XANES. J Phys (Paris) C8 47:49–54

Garrat RC, Evans RE, Hasnain SS, Lindley P (1986) An extended X-ray absorption fine structure investigation of diferric transferrins and their iron-binding fragments. Biochemistry 233:479–484

Garrat RC, Evans R, Hasnain SS, Lindley F (1991) XAFS studies of chicken dicupric ovotransferrin. Biochem J 233:151–155

Grossmann JG, Neu M, Evans RW, Lindley PF, Appel H, Hasnain SS (1993) Metal-induced conformational changes in transferrins. J Mol Biol 229:585–590

Grossmann JG, Crawley JB, Strange RW, Patel KJ, Murphy LM, Neu M, Evans RW, Hasnain SS (1998) The nature of ligand-induced conformational change in transferrin in solution. An investigation using X-ray scattering, XAFS and site-directed mutants. J Mol Biol 279:461–472

Harris WR (1983) Thermodynamic binding constants of the zinc–human serum transferrin complex. Biochemistry 22:3920–3926

Harris WR (1986) Estimation of the ferrous transferrin binding constant based on thermodynamic studies of nickel–transferrin. J Inorg Biochem 27:41–52

Hasnain SS, Hodgson KO (1999) Structure of metal centres in proteins at subatomic resolution. J Synchrotron Radiat 6:852–864

Hirose J, Fujiwara H, Magarifuchi T, Iguti Y, Iwamoto H, Kominami S, Hiromi K (1996) Copper binding selectivity of N and C sites in serum and ovotransferrin. Biochim Biophys Acta 1296:103–111

Kretchmar SA, Raymond KN (1986) Biphasic kinetics and temperature dependence of iron removal from transferrin by 3,4-LICAMS. J Am Chem Soc 108:6212–6218

Kurokawa H, Mikami B, Hirose M (1995) Crystal structure of diferric hen ovotransferrin at 2.4 Å resolution. J Mol Biol 254:196–199

Legrand D, Mazurier J, Montreuil J, Spik G (1988) Structure and spatial conformation of the iron-binding sites of transferrins. Biochimie 70:1185–1195

Lindley PF, Bajaj M, Evans RW, Garrat RC, Hasnain SS (1993) The mechanism of iron uptake by transferrin: the structure of an 18 kDA NII-domain fragment from duck ovotransferrin at 2.3 Å resolution. Acta Crystallogr Sect D 49:292–304

Macgillivray RTA, Moore SA, Chen J, Anderson BF, Baker H, Luo Y, Bewley M, Smith CA, Murphy MEP, Wang Y, Mason AB, Woodworth RC, Brayer GD, Baker EN (1998) Two high-resolution crystal structures of the recombinant N-lobe of human transferrin reveal a structural change implicated in iron release. Biochemistry 37:7919–7928

Mizutani K, Yamashita H, Kurokawa H, Mikami B, Hirose M (1999) Alternative structural state of transferrin. The crystallographic analysis of iron loaded but domain-opened ovotransferrin N-lobe. J Biol Chem 274:10190–10194

Muller JE, Jepsen O, Wilkins JW (1982) X-ray absorption spectra: K-edges of 3d transition metals, L-edges of 3d and 4d metals and M-edges of palladium. Solid State Commun 42:365–368

Natoli CR, Benfatto M, Brouder C, Ruiz Lopez MF, Foulis DL (1990) Multi-channel multiple scattering theory with general potentials. Phys Rev B 42:1944–1968

Roskams AJ, Connor JR (1990) Aluminum access to the brain: a role for transferrin and its receptor. Proc Natl Acad Sci USA 87:9024–9027

Soldatov AV, Ivanchenko TS, Della Longa S, Kotani A, Iwamoto Y, Bianconi A (1994) Crystal-structure effects in the Ce L_3-edge X-ray absorption spectrum of CeO_2: multiple scattering resonances and many-body final states. Phys Rev B 50:5074–5080

Strange RW, Blackburn NJ, Knowles PF, Hasnain SS (1987) X-ray absorption spectroscopy of metal–histidine coordination in metalloproteins. Exact simulation of the EXAFS of tetrakis(imidazole)copper(II) nitrate and other copper–imidazole complexes by the use of a multiple scattering treatment. J Am Chem Soc 109:7157–7162

Williams J (1975) Iron-binding fragments from the carboxyl-terminal region of hen ovotransferrin. Biochem J 149:237–244

Williams J (1982) The evolution of transferrins. Trends Biochem Sci 7:394–397

Woolery GL, Powers L, Winkler M, Solomon EI, Lerch K, Spiro TO (1984) Extended X-ray absorption fine structure study of the coupled binuclear copper active site of tyrosinase from *Neurospora crassa*. Biochim Biophys Acta 788:155–161

Zapolski EJ, Princiotto JV (1980) Binding of iron from nitrilotriacetate analogues by human transferrins. Biochemistry 19:3599–3603